Commensurability and finite size effects in lattice simulations of diblock copolymers†

Akash Arora, David C. Morse, Frank S. Bates and Kevin D. Dorfman*

Lattice Monte Carlo (MC) simulations provide an efficient method for exploring the structure and phase behavior of block polymer melts. However, the results of such simulations may differ from the equilibrium behavior of a hypothetical infinite system as a consequence of the finite size of the simulation box. Standard finite-size scaling techniques cannot be employed to remove the effects of a small system size due to incommensurability between the ordered structure domain spacing and the periodicity of the simulation box. This work describes a systematic approach to estimating the equilibrium domain spacing in lattice MC simulations of symmetric diblock copolymers, and thereby minimize the effects of incommensurability. Results for simulations with commensurate simulation boxes, which are designed to be commensurate with the preferred lattice periodicity but contain different numbers of unit cells, show that once the effects of incommensurability are removed, the effects of finite size alone are relatively small.

1 Introduction

Block copolymers self-assemble to form a variety of ordered structures with the periodic length dictated by the degree of polymerization, N.[1] The resulting materials have been instrumental in the development of several emerging technologies including nanostructured membranes,[2] photonic crystals,[3] magnetic storage media,[4] and silicon capacitors.[5,6] Many of these applications require ordered structures with characteristic dimensions as small as possible.[7] Achieving the smallest feature sizes requires low molecular weight (small N) block polymers and a correspondingly large Flory–Huggins interaction parameter, χ, such that the segregation strength, χN, is high enough to result in the formation of ordered structures. Recent work with relatively small diblock copolymers, unencumbered by kinetic limitations to transitions between ordered states, has revealed unexpected phase complexity. For example, relatively short, high χ, compositionally asymmetric diblock copolymers of poly(isoprene-b-lactide), have produced a Frank–Kasper σ phase comprised of a large tetragonal unit cell containing 30 particles.[8] The σ phase nucleates from a body-centered cubic (BCC) phase by breaking symmetry, resulting in five different populations of particle volumes in a single unit cell.[9] The time required to transform from the BCC to σ phases is many hours, even for

such short polymers, underscoring the need for computationally efficient algorithms with which to model such behavior.

Quantitatively describing the thermodynamics of small block copolymers is an outstanding problem in polymer physics. Mean-field theory[10] predicts that a melt of infinitely long ($N \rightarrow \infty$) volumetrically symmetric ($f = 1/2$) AB diblock copolymers undergoes a continuous second-order phase transition at $\chi N = 10.5$ that transforms the isotropic disordered phase to an ordered lamellar structure, known as the order–disorder transition (ODT). However, it has been shown both theoretically[11] and experimentally[12–14] that symmetric AB diblocks of finite molecular weight belong to the Brazovskii class,[15] for which composition fluctuations qualitatively alter the character of the transition, changing it to a weakly first-order transition.[13] Fredrickson and Helfand[11] adapted the seminal work of Brazovskii[15] to account for fluctuations in block copolymers, and showed that corrections to mean-field theory are controlled by dimensionless parameter $\bar{N} = N(\rho_0 b^3)^2$, where ρ_0 is the monomer density, and b is the statistical segment length, and obtained corrections that decrease with increasing $\bar{N}$. $\bar{N}$, an invariant degree of polymerization, characterizes the degree of overlap between chains. The Fredrickson–Helfand theory has been successful in predicting certain qualitative aspects of fluctuating disordered diblock copolymers but is expected to be accurate only in the limit of very high molecular weight, and has been shown to give unphysical results when $N < 10^3$.[16] Recently, an approach that more realistically addresses practical molecular weights, referred to as renormalized one-loop (ROL) theory,[17,18] has been developed. The ROL theory seems to account for the structure factor in the disordered phase for much smaller values of N, and in

Department of Chemical Engineering and Materials Science, University of Minnesota–Twin Cities, 421 Washington Ave. SE, Minneapolis, Minnesota 55455, USA. E-mail: dorfman@umn.edu

† Electronic supplementary information (ESI) available: Structural and thermodynamic properties of incommensurate and commensurate systems. See DOI: 10.1039/c5sm00838g

particular for the type of short diblock copolymers considered here ($N < 100$). However, the ROL theory does not provide any information about the ODT and the properties in the ordered phase.

In the absence of predictive theory, computer simulations emerge as an attractive approach to study fluctuation effects in block copolymers.[19,20] In particular, lattice Monte Carlo (MC) simulations are a very efficient means to predict the ODT in block copolymers,[21–24] which are generally more efficient than off-lattice models.[25–27] The savings in computational time becomes particularly important when both equilibration and production periods are required at numerous temperatures (or values of χ), and in simulations that require long temperature (or χ) sweeps to identify a transition. The efficiency of MC simulations may be further enhanced by employing advance sampling techniques such as parallel tempering[28,29] and reweighting schemes,[30] though we do not employ these techniques here.

Despite much prior work, the accuracy of the ODT predicted from MC simulations is still not completely understood. This stems in part from the fact that, in the simulation, the system is constrained within a finite box of length L. This shifts the transition away from its true value, *i.e.*, the value that would be obtained in the thermodynamic limit, $L \to \infty$. This finite size effect is particularly severe for transitions involving spatially periodic ordered phases, because the finite size of the box can constrain the domain spacing of the ordered structure to a value that is not equal to the preferred domain spacing that would be obtained for an infinite system. This incommensurability between the periodicity of the simulation box and that of the ordered structure also prevents the use of standard finite-size scaling techniques that were designed for phase transitions between spatially homogenous phases.[31] In off-lattice models, this incommensurability can sometimes be avoided by using a deformable box that can automatically adjust to be commensurate with the preferred domain spacing.[32] However, in the case of lattice models, this problem of incommensurability has not yet been solved.

In this work, we address the issues related to finite size effects and commensurability in MC simulations with the lattice model for symmetric diblock copolymers. We estimate the preferred domain spacing by comparing results of simulations of varied simulation box size L, and use this result to identify nearly-commensurate systems. Simulation results for a series of nearly commensurate systems characterized by the same layer spacing but different numbers of layers are then compared to elucidate any remaining finite size effects and to estimate physical properties in the thermodynamic limit.

2 Simulation method

The simulation methodology and features reported here are based on the algorithm developed by Matsen and coworkers.[24,33,34] The system consists of n symmetric AB diblock copolymer chains that are placed on an FCC lattice having $V = L^3/2$ sites. Approximately 20% of the available sites are left vacant, to allow mobility.

Simulations are implemented using the Metropolis Monte Carlo method with four different types of moves: reptation, crankshaft, block-exchange, and chain-reversal.[24] Only nearest neighbor interactions are considered, with the strength of each interaction given by $\varepsilon_{AB} > 0$ for neighboring sites occupied by dissimilar (AB) monomer pairs, and no interaction ($\varepsilon_{AA} = \varepsilon_{BB} = 0$) for sites occupied by similar (AA or BB) monomer pairs, as done in some recent simulations.[32]

Throughout this paper, results are discussed and plotted in terms of a simple "bare" Flory–Huggins parameter, given by $\chi \equiv z\varepsilon_{AB}/k_BT$, where $z = 12$ is the lattice coordination number. Because we are interested only in characterizing the behavior of a simple model, and not in comparing different models to each other or to experiments, no attempt is made here to define an "effective" interaction parameter suitable for such comparisons, as done in some recent simulations.[32] Also, the results predicted by this lattice model recently have been compared with the theoretical predictions,[16] which are omitted here for brevity.

To identify the ODT, the system is cooled by increasing χN in steps of constant size $\Delta(\chi N)$, increasing χN from $\chi N = 0$ to values large enough to induce a transition to an ordered structure. The resulting ordered structure is then heated (*i.e.* χN is reduced) in steps of the same size, until $\chi N = 0$. During both the cooling and the heating runs, the starting configuration at any value of χN is obtained from the final configuration at the previous value of χN. At each value of χN, 8×10^4 Monte Carlo steps (MCS) per monomer are performed for equilibration, followed by 8×10^4 MCS per monomer as a production period before implementing the next step of $\Delta(\chi N)$. Samples are taken at an interval of 160 MCS per monomer during the production period to calculate ensemble averages.

We calculate the number of AB contacts, n_{AB}, which enables us to compute the internal energy of the system,

$$\langle U \rangle = \varepsilon_{AB} \langle n_{AB} \rangle. \tag{1}$$

We also calculate the heat capacity based on fluctuations in the internal energy,

$$C_V = \frac{\partial U}{\partial T} = \frac{\langle U^2 \rangle - \langle U \rangle^2}{k_B T^2}. \tag{2}$$

In order to find the orientation of the lamella and consequently the domain spacing, we compute the structure factor,

$$S(\mathbf{q}) = \frac{1}{V} \sum_{ij} \left[\langle \sigma_i \sigma_j \rangle - \langle \sigma_i \rangle^2 \right] \exp\left[i\mathbf{q} \cdot \mathbf{r}_{ij} \right], \tag{3}$$

where $\sigma_i = 0$, 1, or -1 is the lattice occupancy of the site depending on whether it contains a vacancy, a monomer of type A, or a monomer of type B, respectively. The vector, $\mathbf{r}_{ij}(=\mathbf{r}_i - \mathbf{r}_j)$, is the position vector from site i to site j. The wave vector, $\mathbf{q}$ can only take on values

$$\mathbf{q} = \frac{2\pi}{L}(hkl), \tag{4}$$

where (hkl) are integers. For each case investigated in this work, eight statistically independent simulations were conducted.

3 Results and discussion

All the results presented in this paper were obtained for chains of length $N = 20$. However, the approach is general and can be easily applied to other chain lengths, and to other models. The simulation procedure described in the previous section provides a direct method to identify the ODT. Fig. 1 shows the average number of AB contacts for both cooling and heating runs, which determines the average internal energy (eqn (1)). The hysteresis loop evident in this plot is consistent with the presence of a first-order phase transition. As expected, the discontinuity at each end of the hysteresis loop coincides with a spike in the heat capacity (Fig. S-1 in the ESI†).

In order to assess the role of finite size effects, a relevant thermodynamic property (*e.g.* $(\chi N)_{ODT}$) or structural features (*e.g.* $S(q)$) must be computed for a range of system sizes. If there were no commensurability effects, then these properties would be expected to increase or decrease monotonically with inverse system size $1/L$, allowing the value in the thermodynamic limit to be inferred by extrapolation to $L = \infty$.

As a first step toward estimating $(\chi N)_{ODT}$, we examined the behavior of the $\langle n_{AB} \rangle$ near the ODT for six different system sizes, ranging from $L = 24$ to $L = 64$ with $\Delta L = 8$. As seen in the ESI† (Fig. S-2, ESI†), neither the positions nor widths of hysteresis loops vary monotonically with L. This non-monotonic behavior is not limited to the hysteresis loops, but also is clear from the evolution of the structure factor in the disordered phase (Fig. S-3, ESI†) and the structural metrics for the blocks (Fig. S-4, ESI†). Our observations agree with the conclusion of Micka and Binder[31] that the incommensurability between the lattice periodicity and the domain spacing prevents the appearance of any simple monotonic variation of physical properties with L. As a result, standard procedure to study finite size effects upon transitions between homogeneous phases cannot be applied in this case.
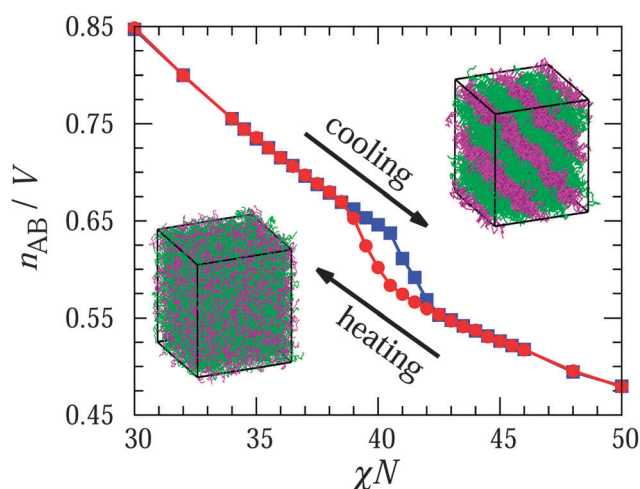
To minimize the effects of incommensurability, we must thus first estimate the preferred domain spacing, and then design simulations using nearly-commensurate simulations boxes that are designed to contain integral number of nearly unstrained lamellar layers. We observe that simulations using boxes of different size L spontaneously order in different orientations. For each box size L, the preferred orientation at the ODT appears to be reproducible. Our analysis is based on the hypothesis that the orientation in each box is chosen so as to minimize the difference between the layer spacing and the preferred layer spacing that would be obtained in an infinite system. Each allowed orientation can be associated with a primary wavevector **q** given by eqn (4). Because **q** can only take on discrete values in a finite simulation cell, the corresponding layer spacing d can also only have discrete values, given by

$$d = \frac{2\pi}{|\mathbf{q}|} = \frac{L}{\sqrt{h^2 + k^2 + l^2}}, \qquad (5)$$

with integer values of (hkl).

Fig. 2 shows our results for the domain spacing d at the ODT for systems of size $L = 28$–60, for all even L. The red symbols show the allowed values of d, as given by eqn (5). The values are clustered around $d \simeq 14$ but exhibit jumps between neighboring values of L that, in the absence of more detailed analysis, might appear to be erratic. Upon comparison of actual and allowed values, however, it becomes clear that these data are consistent with our hypothesis that the system always chooses an orientation that optimizes d. Wherever there are sudden spikes in the observed d spacing, as occur at $L = 36$, 38 and 54, it is because there is no choice of values for the integers (hkl) for those values of L that would yield a value of d that is closer to an apparent optimum value of approximately $d \simeq 14$. The reproducibility of this behavior suggests that these systems have sufficient freedom

Fig. 1 Number of AB contacts per simple cubic site, $\langle n_{AB} \rangle / V$, as a function of segregation strength, χN, for both a cooling (blue) and heating (red) run, where $\Delta(\chi N) = 0.5$. The insets show snapshots of the disordered phase (left) and the lamellar structure (right) at $\chi N = 0$ and 43, respectively.
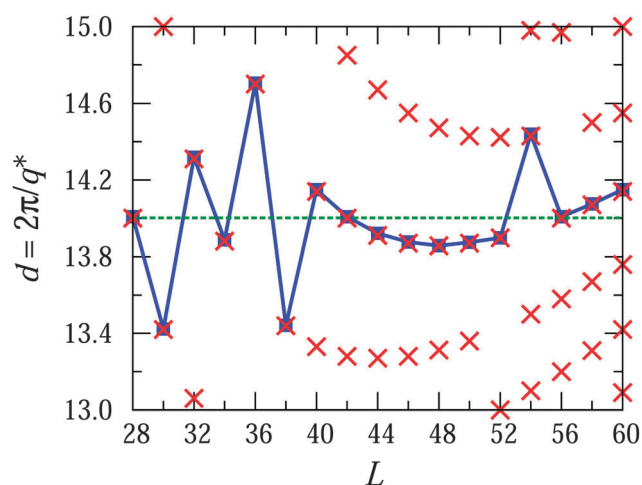

Fig. 2 Domain spacing in the ordered phase as a function of system size. The blue squares are the domain spacing from the simulations, with the blue line drawn to guide the eye. The green dashed line is the average value of the domain spacings from the simulations. The red cross symbols show all nearby allowed values of d for a given L calculated using eqn (5).

during the process of spontaneous ordering to choose an optimum orientation.

If we assume that the system always choose an orientation that minimizes the difference between d and some unknown optimal value d_{eq}, we can also use these data to put upper and lower bounds on d_{eq}. For each L, we obtain a lower bound from the midpoint between the observed value of d and the next lower allowed value, and an upper bound from the midpoint between the actual value and the next higher allowed value. The overall bounds on our estimate of d_{eq} are given by the maximum lower bound and the minimum upper bound. For these data, the tightest lower bound is obtained from $L = 60$, which yields $d_{eq} > 13.9$, while the tightest upper bound is provided by $L = 50$, which yields $d_{eq} < 14.2$, leaving an uncertainty of approximately 2%.

In order to estimate the effects of finite size alone on systems with the same layer spacing, we have compared results of simulations of systems with lattice sizes $L = 28$, 42, 56, and 70 that are all found to produce lamellar phases with $d = 14$. Since these systems have a common layer spacing $d = 14$ that lies very close to the (unknown) optimum value, we refer to these systems as "nearly commensurate". Snapshots of the lamellar phase formed by this series of nearly-commensurate systems are presented in Fig. 3. As expected, the system sizes $L = 28$, 42, 56, and 70 contain 2, 3, 4 and 5 lamellar layers, respectively. Note that Fig. 3 shows the lamellae oriented along the principal directions only. However, in some of several independent simulations, lamellae were found to form with indices $(\bar{1}22)$ and $(04\bar{3})$ for the systems $L = 42$ and $L = 70$, respectively, which in these cases give rise to ordered phases with exactly the same layer spacing but different orientation (Fig. S-5, ESI†).

Having obtained the commensurate systems, we are now in a position to address the consequences of finite size effects. Fig. 4 compares the hysteresis in the internal energy for these
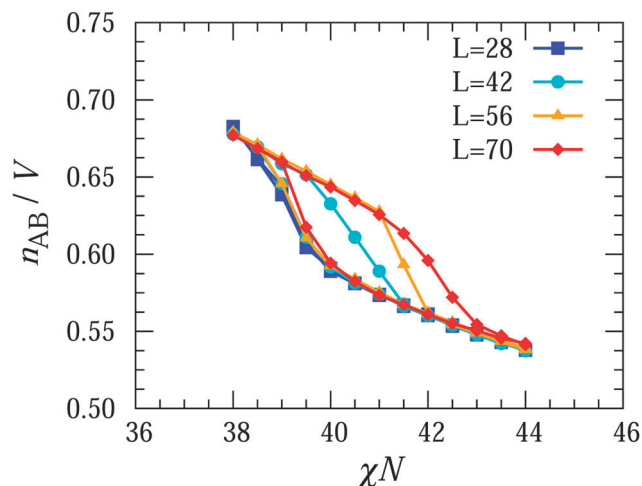

Fig. 4 Hysteresis in the internal energy for the four commensurate systems. The data correspond to constant cooling and heating step sizes of $\Delta(\chi N) = 0.5$.

four nearly-commensurate systems. As expected, the width of the hysteresis loop increases with an increase in the lattice size. However, it is important to note that the variations in this width result almost entirely from changes in the cooling branch; within the precision of the simulations, the heating branch of the hysteresis loop remains unaffected. This observation also is evident in the position of the spike in the heat capacity, which for the cooling run shifts to higher values of χN with increasing L, while remaining at fixed χN for all L in the heating runs (Fig. S-6, ESI†). This behavior is intuitive as explained by Matsen and coworkers:[24] larger system sizes, with larger total energy, require longer time to nucleate an ordered phase, thereby increasing the degree of supercooling. This is analogous to what is found in practice when heating and cooling real substances through melting and fusion phase transitions. Thus increasing the rate of temperature change has a more dramatic impact on the extent of supercooling of the liquid than on the degree of superheating of the crystalline state. These results demonstrate that the ODT lies very close to the apparent ODT obtained from the heating branch and does not move significantly upon changing the size of the lattice. In other words, the ODT determined with the lattice Monte Carlo simulation model during heating does not suffer from artifacts associated with a finite simulation box. For the example considered here, $N = 20$, we conclude that $(\chi N)_{ODT} \simeq 40$.

Here we note that Matsen and coworkers[24,34] have reported essentially the same value of $(\chi N)_{ODT}$ for $N = 20$, with the stated expectation that finite-size effects should not be too significant. Plots of hysteresis obtained from commensurate and incommensurate simulations (Fig. S-2, ESI†) demonstrate that the computed lamella-to-disorder transition values are randomly clustered around a mean value $(\chi N)_{ODT} = 40$ for different L. However, it is important to note that the associated thermodynamic properties display non-monotonic variations with L and therefore definite conclusions cannot be drawn regarding finite-size effects. By selecting only the commensurate systems, we have been able to show conclusively that finite size effects do not adversely affect what we report here.
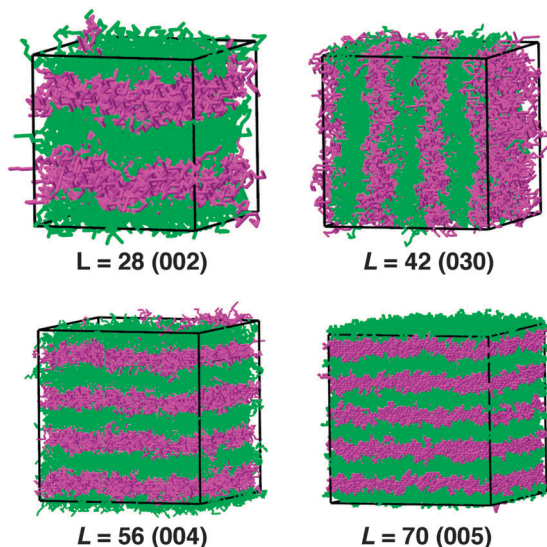

Fig. 3 Snapshots of the lamellar phase formed by "nearly-commensurate" systems; $L = 28$, 42, 56 and 70. These snapshots were taken at $\chi N = 43$. Depictions of the lamellae formed for $L = 42$ in the $(\bar{1}22)$ direction and for $L = 70$ in the $(04\bar{3})$ direction are provided in Fig. S-5 (ESI†).
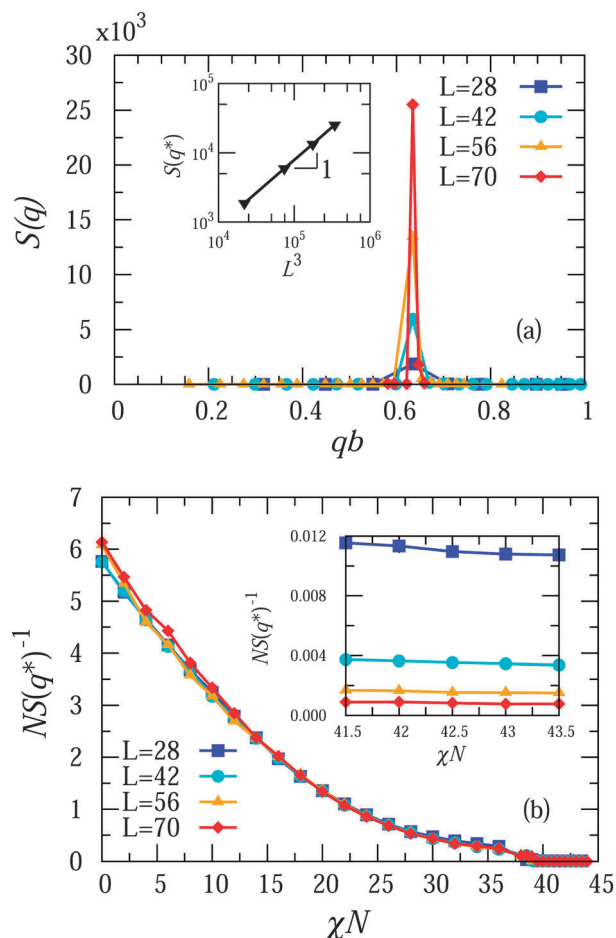
Fig. 5 (a) Structure factor, $S(q)$, as a function of the non-dimensional wave vector, qb, for the four commensurate systems in the ordered phase at $\chi N = 43$. The inset shows the scaling between the peak in structure factor, $S(q^*)$, and system volume, L^3. (b) Inverse of the peak in the structure factor, $NS^{-1}(q^*)$, as a function of the segregation strength, χN, for the complete heating run. The inset shows the variation of inverse of the peak of the structure factor in the ordered phase.

In addition to $(\chi N)_{ODT}$, we have calculated several other properties, such as the chain dimensions and collective structure factor, to demonstrate that all the structural features are systematically accounted for by choosing commensurate system sizes. As an illustrative example, Fig. 5(a) shows the structure factor in the ordered lamellar phase at $\chi N = 43$ for all four commensurate systems, where a Bragg-like peak dominates the structure factor in the ordered phase. The peak height for the commensurate systems increases monotonically with the lattice size in direct proportionality to the volume of the system, L^3, and the peak width decreases inversely with L^3, as shown in the inset to Fig. 5(a). This result confirms the scaling behavior expected in the ordered phase.[31]

Fig. 5(b) shows the evolution of the inverse of the peak height, $S(q^*)^{-1}$, for the complete heating run. Note that the disordered phase is isotropic, so the structure factor in the disordered phase is calculated as a spherical average for a constant length of wavevector, $|\mathbf{q}|$. Fig. 5(b) shows that the peak height of the structure factor is independent of L in the disordered phase.

However, in the ordered phase, the inverse of the peak height is lowest for the largest system as shown in the inset of the Fig. 5(b), in agreement with Fig. 5(a). Taken together, these results confirm that finite size effects do not appreciably influence the structure factor in either phase.

4 Conclusion

We have presented a systematic study of finite size effects in lattice Monte Carlo simulations of symmetric diblock copolymers. Incommensurability between the lamellar domain spacing and the periodicity of the lattice produces a non-monotonic variation in the thermodynamic and structural properties with system size. In order to estimate the preferred domain spacing we conducted simulations with multiple choices for the system size. The results are consistent with the hypothesis that the system always chooses a lamellar orientation that minimizes the difference between the layer spacing and some preferred equilibrium value, and allow us to estimate the preferred value.

Our results for the ODT are sensitive to the effects of finite simulation box size upon the free energies of both the disordered and ordered phases. In the disordered phase, because there is a finite correlation length, finite size effects can be made exponentially small by making the box larger than the correlation length. In any ordered phase, because there is infinitely long range periodic order, the boundaries can always "communicate" via the imposition of a strain that propagates through the entire simulation box. This strain can be completely removed, however, by making the periodic simulation unit cell commensurate with the preferred domain spacing of the ordered structure. In a finite but perfectly commensurate simulation cell, there also would be shorter range correlations for fluctuations of the composition field about its average, i.e., for the fluctuations that are measurable experimentally as the diffuse scattering that is superimposed on the Bragg peaks. In order to suppress such effects in an ordered phase, the simulation cell must both be commensurate and large enough to suppress finite size effects arising from remaining composition fluctuations about the average periodic field. Even if the box is not perfectly commensurate, simulations on boxes with the same degree of strain (i.e., the same ratio of the imposed layer spacing to the preferred value) should yield equivalent results if the box is large enough to avoid finite size effects arising from spatially correlated fluctuations about the average. The close agreement that we get for values of the ODT for nearly-commensurate systems having same layer spacing but different integer numbers of layers demonstrates that finite size effects arising from spatially correlated fluctuations are already small in both phases for the box sizes considered here.

We have also demonstrated that, for nearly-commensurate systems, the dependence of the width of the hysteresis loop with changes in system size at constant heating and cooling rate are primarily the result of increases in the value of χN at which the system spontaneously orders upon cooling. The values of χN at which the system melts at a given heating rate appear to be

almost independent of system size, when comparing systems with the same layer spacing. This suggests that the true ODT lies close to the apparent melting transition.

The approaches described in this paper are general, and can be applied to other choices of simulation model and chain length. By performing a few simulations at small L for some value of N (and, in principle, f) and obtaining the selected domain spacing at these values of L, we can quickly estimate the preferred domain spacing, and then design nearly commensurate systems for further investigation, thereby circumventing a potentially expensive, trial-and-error process. Though this strategy can be applied to either lattice or off-lattice simulations, it is particularly useful for lattice simulations because of the inapplicability of approaches that use a deformable unit cell. We thus anticipate that the strategy outlined here will increase the appeal of lattice simulations of block polymers, and will be useful in quantifying the role of fluctuations in the phase behavior of diblock copolymers.

Acknowledgements

References

1 F. S. Bates, *Science*, 1991, **251**, 898–905.
2 E. A. Jackson and M. A. Hillmyer, *ACS Nano*, 2010, **4**, 3548–3553.
3 A. M. Urbas, M. Maldovan, P. DeRege and E. L. Thomas, *Adv. Mater.*, 2002, **14**, 1850–1853.
4 J. Y. Cheng, C. Ross, V.-H. Chan, E. L. Thomas, R. G. Lammertink and G. J. Vancso, *Adv. Mater.*, 2001, **13**, 1174–1178.
5 F. S. Bates and G. H. Fredrickson, *Phys. Today*, 1999, **52**, 32–38.
6 S. O. Kim, H. H. Solak, M. P. Stoykovich, N. J. Ferrier, J. J. de Pablo and P. F. Nealey, *Nature*, 2003, **424**, 411–414.
7 M. P. Stoykovich and P. F. Nealey, *Mater. Today*, 2006, **9**, 20–29.
8 S. Lee, M. J. Bluemle and F. S. Bates, *Science*, 2010, **330**, 349–353.
9 S. Lee, C. Leighton and F. S. Bates, *Proc. Natl. Acad. Sci. U. S. A.*, 2014, **111**, 17723–17731.
10 L. Leibler, *Macromolecules*, 1980, **13**, 1602–1617.

11 G. H. Fredrickson and E. Helfand, *J. Chem. Phys.*, 1987, **87**, 697–705.
12 F. S. Bates, J. H. Rosedale, G. H. Fredrickson and C. J. Glinka, *Phys. Rev. Lett.*, 1988, **61**, 2229.
13 F. S. Bates, J. H. Rosedale and G. H. Fredrickson, *J. Chem. Phys.*, 1990, **92**, 6255–6270.
14 S. Lee, T. M. Gillard and F. S. Bates, *AIChE J.*, 2013, **59**, 3502–3513.
15 S. Brazovskii, *J. Exp. Theor. Phys.*, 1975, **41**, 85.
16 J. Glaser, P. Medapuram, T. M. Beardsley, M. W. Matsen and D. C. Morse, *Phys. Rev. Lett.*, 2014, **113**, 068302.
17 P. Grzywacz, J. Qin and D. C. Morse, *Phys. Rev. E: Stat., Nonlinear, Soft Matter Phys.*, 2007, **76**, 061802.
18 J. Qin and D. C. Morse, *Phys. Rev. Lett.*, 2012, **108**, 238301.
19 T. Pakula, K. Karatasos, S. Anastasiadis and G. Fytas, *Macromolecules*, 1997, **30**, 8463–8472.
20 Q. Wang, P. F. Nealey and J. J. de Pablo, *Macromolecules*, 2002, **35**, 9563–9573.
21 H. Fried and K. Binder, *J. Chem. Phys.*, 1991, **94**, 8349–8366.
22 A. Hoffmann, J.-U. Sommer and A. Blumen, *J. Chem. Phys.*, 1997, **106**, 6709–6721.
23 T. Gemma, A. Hatano and T. Dotera, *Macromolecules*, 2002, **35**, 3225–3237.
24 O. Vassiliev and M. Matsen, *J. Chem. Phys.*, 2003, **118**, 7700–7713.
25 M. Müller and K. C. Daoulas, *J. Chem. Phys.*, 2008, **128**, 024903.
26 F. A. Detcheverry, D. Q. Pike, P. F. Nealey, M. Müller and J. J. de Pablo, *Phys. Rev. Lett.*, 2009, **102**, 197801.
27 K. Binder and D. Heermann, *Monte Carlo simulation in statistical physics: an introduction*, Springer Science & Business Media, 2010.
28 Q. Yan and J. J. de Pablo, *J. Chem. Phys.*, 1999, **111**, 9509–9516.
29 D. J. Earl and M. W. Deem, *Phys. Chem. Chem. Phys.*, 2005, **7**, 3910–3916.
30 J. D. Chodera, W. C. Swope, J. W. Pitera, C. Seok and K. A. Dill, *J. Chem. Theory Comput.*, 2007, **3**, 26–41.
31 U. Micka and K. Binder, *Macromol. Theory Simul.*, 1995, **4**, 419–447.
32 P. Medapuram, J. Glaser and D. C. Morse, *Macromolecules*, 2015, **48**, 819–839.
33 M. W. Matsen, G. H. Griffiths, R. Wickham and O. Vassiliev, *J. Chem. Phys.*, 2006, **124**, 024904.
34 T. Beardsley and M. W. Matsen, *Eur. Phys. J. E: Soft Matter Biol. Phys.*, 2010, **32**, 255–264.